ISSN (Online) 2395-2717

International Journal of Engineering Research in Electrical and Electronic Engineering (IJEREEE)
Vol 3, Issue 3, March 2017

Enhancement of Droop Characteristics with Synchronous Power Controller for Renewable Power Generation

[1] O. Hemakesavulu, [2] Dr. M. Padmalalitha [3]V. Vidyavani
[1] Associate Professor [2] Professor & HOD [3]P. G. Scholar
[1][2][3] Annamacharya Institute of Technology And Sciences (Autonomous), Rajampet, Kadapa dist, A.P, India.

Abstract: **— The increasing amount of renewable power generation systems is a challenging issue for the control and operation of the electrical networks. One of the main issues is their lack of inertia, which is becoming a greater problem as much as the share of the power plants based on traditional synchronous generators gets reduced. In this regard, the new grid codes ask these plants to provide new functionalities such as the frequency support and inertia emulation. In this project, a synchronous power controller for grid-connected converters is proposed as a good solution for the renewable generation systems. It provides inertia, damping, and flexible droop characteristics. Different from the faithful replication of the swing equation of synchronous machines, an alternative control structure is proposed, by which the damping and inherent droop slope can be configured independently to meet the requirements in both dynamics and frequency regulations. Simulation results are obtained using MATLAB/Simulink shows the performance of the proposed control strategy.**

Index Terms: **— DC–AC power conversion, inertia emulation, power generation control, synchronous power controller.**

I. INTRODUCTION

Traditional generation plants based on renewable energy sources (RES) act as grid-feeding systems, which deliver the maximum power from the primary source to the grid. As much as the penetration of the RES generation plants increases, the insufficient inertia in the whole network could undermine its operating stability. Therefore, the control objectives and dynamics of the grid-connected converters need to be adjusted to take more responsibilities in grid supporting issues, like as inertia emulation, frequency regulation and voltage support.

A solution to improve the dynamics of the converters is to specify the properties of the grid-connected converters in such a way that it acts like a synchronous generator (SG).This trend is initiated by the fact that conventional grid synchronization algorithm like Phase-locked loop (PLL) presents not inertia characteristics.

A control implementation scheme for emulation of SG is proposed, in which the loop filter of the conventional PLL is modified. Another implementation strategy for emulating SG is proposed, in which PLL is substituted by an active power synchronization loop. Even though this strategy has shown advantages in the interconnection of weak ac grids, the inertia and oscillation damping are not specifically addressed, and it has to be switched to a PLL-based vector current control.

Further a synchronous power controller presenting inertia and damping characteristics, and particularly a virtual admittance structure is proposed. In this the inertia can also be implemented in the micro grid droop controller.

The above mentioned designs incorporate the swing equation inherently. Compared with the existing techniques, damping and droop characteristics are particularly addressed, while the inertia feature is maintained.

ISSN (Online) 2395-2717

International Journal of Engineering Research in Electrical and Electronic Engineering (IJEREEE)
Vol 3, Issue 3, March 2017

II. OVERALL CONTROL STRUCTURE

This control scheme is mainly characterized by two blocks, the electromechanical block and the virtual admittance block.

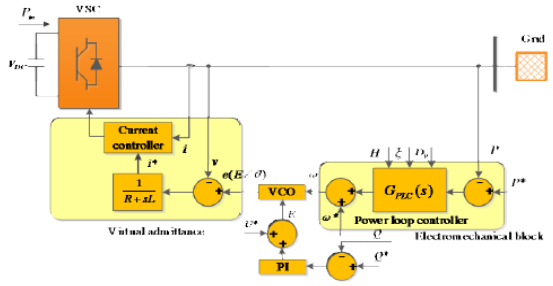

Fig.1: Control scheme of synchronous power controller

The power loop controller generates a virtual synchronous frequency ω, which is then integrated to a phase signal θ. Combining the phase signal θ and the magnitude signal E, the virtual electromotive force e will be generated by the voltage controlled oscillator (VCO).

The virtual admittance structure is shown in Fig.2. It is an emulation of the output impedance of SG.

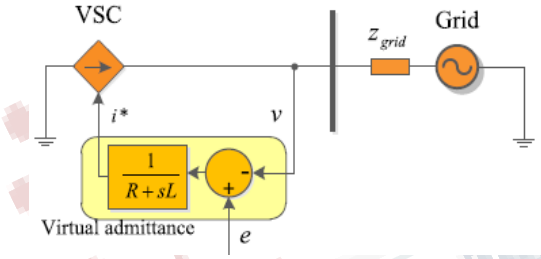

Fig.2: Virtual admittance emulating the electrical characteristics of synchronous machines

According to electrical characteristics of the synchronous machines, the generated active power can be approximated to (1).

$$\Delta P = P_{max}\,\Delta\delta \qquad (1)$$

. The admittance gain is expressed as

$$P_{max} = \frac{EV}{X} \qquad (2)$$

Based on (1), inner control loops can be simply modeled as an admittance gain since it has much faster dynamics compared with outer loops

III. ELECTROMECHANICAL BLOCK

According to the control scheme shown in Fig.1, the active power regulating loop can be modeled as shown in Fig.3, $G_{PLC}(s)$ is designed in this section. Even if the grid voltage angle θgrid is unknown, the synchronous angular speed ω can always be adjusted to accordingly shift the load angleδ. In this way the active power is regulated.

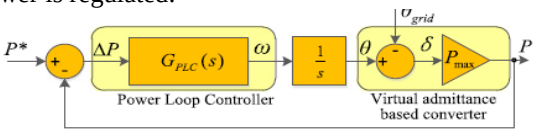

Fig.3: Modeling of active power control loop

A. Mechanical Power Loop (MPL) Controller

The SG swing equation can be expressed as

$$P_{mech} - P_{elec} = \omega_s(Js + D)\omega \qquad (3)$$

Based on the swing equation, the form of $G_{PLC}(s)$ can be designed as shown in (4), which is referenced as MPL controller in this session.

$$G_{PLC}(s) = \frac{1}{\omega_s(Js+D)} \qquad (4)$$

According to (4), the resulting closed-loop transfer function is obtained and shown in

$$\frac{P}{P^*}(s) = \frac{\omega_n^2}{s^2+2\xi\,\omega_n s+\omega_n^2} \qquad (5a)$$

$$\xi = \frac{D}{2}\sqrt{\frac{\omega_s}{JP_{max}}} \qquad (5b)$$

$$\omega_n = \sqrt{\frac{P_{max}}{J\omega_s}} \qquad (5c)$$

Instead of using the moment of inertia J to designate the inertia characteristics, the inertia constant H
is commonly adopted, which is defined as,

$$H = \frac{J\omega_s^2}{2S_N} \qquad (6)$$

According to Fig.3, taking $\omega_g$as the variable while taking P as the function, the transfer function is,.

$$\frac{\Delta P}{\Delta\omega_g}(s) = \frac{-P_{max}(s+2\xi\omega_n)}{s^2+2\xi\,\omega_n s+\omega_n^2} \qquad (7)$$

Droop ratio D_p is given by,

$$D_p = \left(\frac{2\pi}{1000}\right)\left|\frac{\Delta P}{\Delta\omega_g}(0)\right| \text{ kW/hz} \qquad (8)$$

then combining (7) and (8), the intrinsic droop ratio of the MPL controller $D_p(MPL)$ is expressed as

$$D_p(MPL) = \frac{4\pi\xi P_{max}}{1000\,\omega_n} \qquad (9)$$

B. Boundaries of MPL Controller

To further show the restrictions of the MPL controller in parameters tuning, the grid frequency deviation percentage that extracts the full rated power from the converter is used as the indicator of the droop characteristics, which is represented by $\frac{1}{R}$. The relation between D_p and $\frac{1}{R}$ is shown in

ISSN (Online) 2395-2717

International Journal of Engineering Research in Electrical and Electronic Engineering (IJEREEE)
Vol 3, Issue 3, March 2017

$$\frac{1}{R} = \frac{2\pi S_N}{D_p \omega_s} \quad (10)$$

Combining (5c), (6), (9) and (10)

$$\frac{1}{R}(MPL) = \frac{1}{2\xi}\sqrt{\frac{X_{Pu}}{2H\omega_s}} \quad (11)$$

Where, $$X_{Pu} = \frac{S_N}{P_{max}} \quad (12)$$

Equation (11) shows interaction among H,ξ , X_{Pu} and $\frac{1}{R}$. The values of H and X_{Pu} can be pre-fixed respectively and X_{Pu} is set to 0.3 to specify the model. This restriction between ξ and $\frac{1}{R}$ is visualized in Fig.4, where H is specified to 2, 11 and 20 respectively,

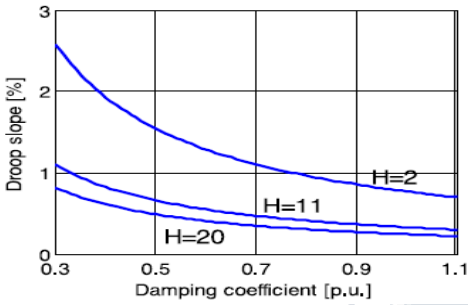

Fig.4: Characteristics between droop slope and damping coefficient

C. Configurable Natural Droop (CND) Controller

Other than the implementation of the swing equation of an SG, a droop branch is included in parallel for controlling the P-f droop slope in steady state, which is shown in Fig.5. The structure of the droop branch is developed in the way that it shares the same denominator with the transfer function of the swing equation. In this manner the order of the power regulating loop does not increase.

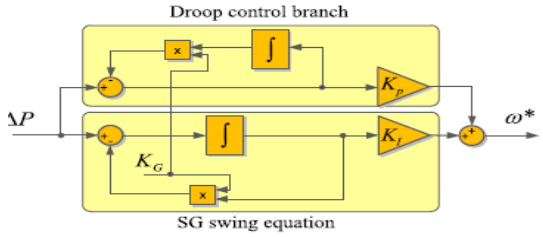

Fig.5: Block diagram of droop controller

The transfer function of the proposed controller is

$$G_{PLC}(s) = \frac{K_p s + K_I}{s + K_G} \quad (13)$$

Substituting the power loop controller block in Fig.3 with the expression (13), the resulting closed loop transfer function is shown in (14a).

$$\frac{P}{P^*}(s) = \frac{(2\xi\omega_n s - K_G)s + \omega_n^2}{s^2 + 2\xi\omega_n s + \omega_n^2} \quad (14a)$$

$$\xi = \frac{P_{max} K_P + K_G}{2\omega_n} \quad (14b)$$

$$\omega_n = \sqrt{P_{max} K_I} \quad (14c)$$

The P-f response of the CND controller is,

$$\frac{\Delta P}{\Delta \omega_g}(s) = \frac{-P_{max}(s + K_G)}{s^2 + 2\xi\omega_n s + \omega_n^2} \quad (15)$$

$$D_{P(CND)} = \frac{2\pi K_G}{1000 K_I} \quad (16)$$

IV. CONTROL PARAMETERS SETTING

The control parameters K_p, K_I and K_G can be clearly set according to the input of D_p, H and ξ. Owing to the explicit link between the controller gains and characteristic parameters, the controller can easily be made adaptive according to the secondary control, and a flexible control paradigm becomes possible.

In order to further tune ξ, the analysis on dynamics is done based on the mathematical transfer functions. A unitary step input is given to the closed loop transfer function (14a), and the influence of ξ on the settling time and overshoot of the time response can be calculated.

The analysis on the relation between ξ and the overshoot of the step response is shown in Fig.6. Since the overshoot of the step response can considerably reflect the damping characteristics of the system, a value greater than 0.7 is proposed as the proper damping value, which can guarantee the overshoot of the step response to be smaller than 25%.

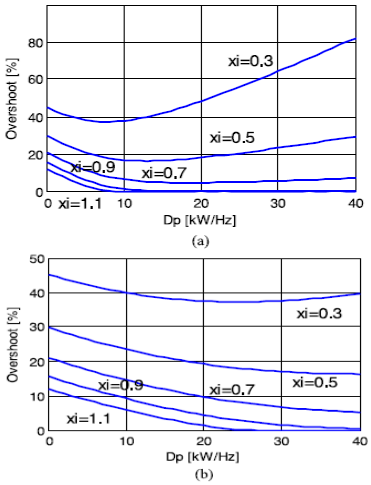

Fig.6: Influence of damping coefficient ξ on the overshoot of power step response: (a) H = 2 and (b) H= 20

ISSN (Online) 2395-2717

International Journal of Engineering Research in Electrical and Electronic Engineering (IJEREEE)
Vol 3, Issue 3, March 2017

V. SIMULINK MODEL OF THE SYSTEM

Simulation studies are conducted for evaluating the performance of the proposed controller in cases of grid-connected converters connecting to weak grids and island operations.

A. Performance When Interfacing Weak Grid

The influence of short circuit ratio (SCR) on the maximum power generation can be easily shown in (17), which defines the per-unit output power of a generation unit is,

$$P_{pu} = SCR.\sin\delta \quad (17)$$

As seen from (17) the generated power will be always smaller than the rated power, when SCR equals to one (which yields an extremely weak grid).

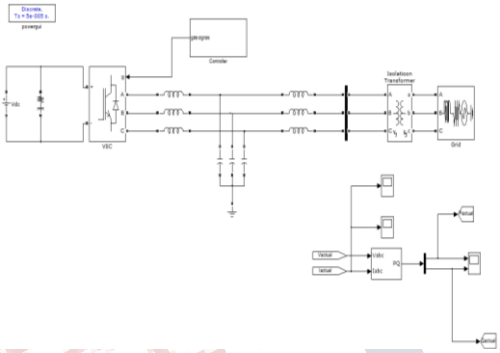

Fig.7: Simulation block diagram when interfacing weak grid

B. Grid Disconnection and Island Operation

The proposed control is featured by the capability of feeding an island similar to synchronous machines. As mentioned before, the reference of reactive power is given by an outer Q-V droop controller.

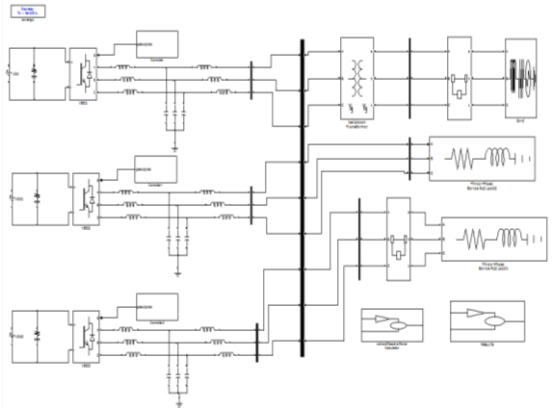

Fig.8: Simulation block diagram under grid disconnection and island operation

Based on the control scheme in Fig. 1 aided by an outer Q-V droop controller, the island operation is possible. It is worth noting that the active power reference will not dominate the active power injection in island operation, instead, the power injection is determined by the virtual admittance and the P-f droop characteristics.

VI. SIMULATION RESULTS

A. Performance When Interfacing Weak Grid

The proposed control is able to inject relatively more power to weak grid under the variation of the power reference, compared with the conventional vector current control accompanied by PLL.

Fig.9.1: Injected current (A)

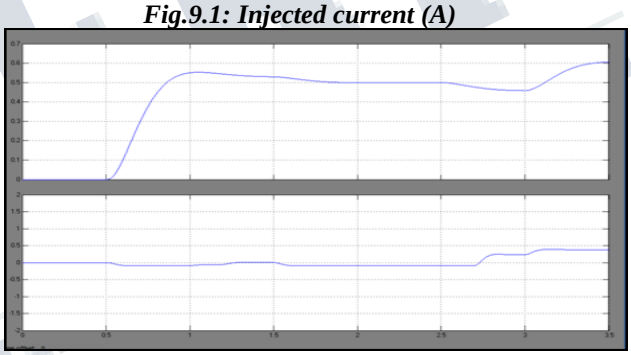

Fig.9.2: Active and reactive power (pu)

Fig.9: Active power step response of the converter connected to weak grid

B. Grid Disconnection and Island Operation

Fig. 8 shows a study case where a 100 kW and two 10 kW converters are connected to the grid in parallel, and serve local loads of 100 kW.

Based on (1), (2) and (12), the power variation of a generation unit can be expressed by,

$$\Delta P_{pu} = \frac{1}{X_{pu}} \Delta\delta \quad (18)$$

According to (18), the virtual reactance for each converter is set to the same per-unit value for a proportional load sharing.

As an initial operation point, the grid connection switch is closed, and the power injection of 3 converters are 8 kW, 7 kW, and 70 kW, respectively, corresponding to 0.8 p.u.,0.7p.u. and 0.7p.u., and the local load is partly fed by the main grid. Two events are considered in the case study. At 1.2 s, a failure in the

ISSN (Online) 2395-2717

International Journal of Engineering Research in Electrical and Electronic Engineering (IJEREEE)
Vol 3, Issue 3, March 2017

main grid appears, while at 1.3 s, the step change of a local load takes place.

Regarding the first event, the local voltage is well maintained when the main grid failure occurs, thanks to the grid forming capability of the proposed control. The local voltage magnitude drop is calculated to be 4.22% as an acceptable value. As a response to this event, all the 3 converters increase the power injection, and the incremental power is all around 0.1 p.u. (with respect to the rated power of each converter). The minor drop of the load power is due to the drop of the grid voltage magnitude

During the second event, 20% of the local load (local load 1) is switched out. The local voltage is well maintained after a short transient, and all the converters decrease the power injection proportional to their rated power.

TABLE-I: Key parameters

Symbol	Definition	Value
V_{DC}	dc-link voltage[V]	640
V_g	Grid phase-phase voltage rms[V]	400
f_g	Grid nominal frequency[Hz]	50
S_N	Nominal power[KW]	10
f_{SW}	Switching frequency[Hz]	10050
ξ	Damping coefficient[p.u]	0.7
R	Virtual resistance[p.u]	0.1
X	Virtual reactance[p.u]	0.3

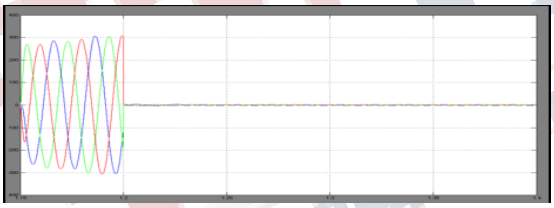

Fig.10.1: Grid voltage (V)

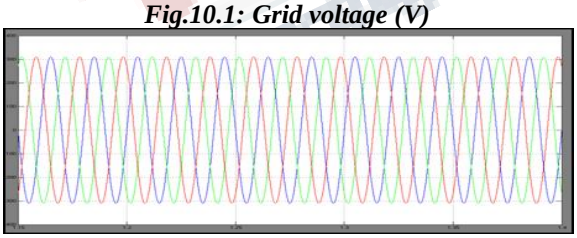

Fig.10.2: .Load voltage (V)

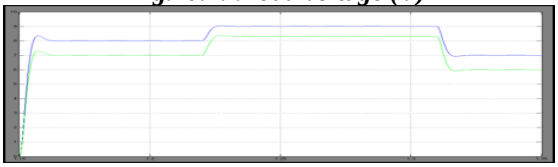

Fig.10.3: Converters 1 and 2 active power (KW)

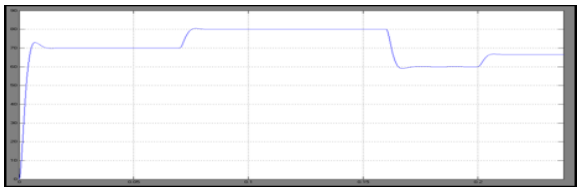

Fig.10.4: Converter 3 active power (KW)

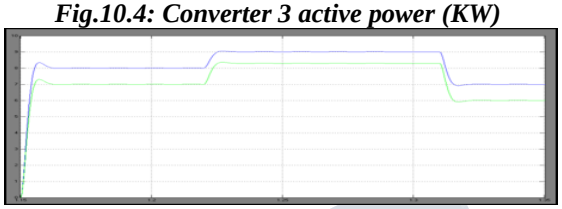

Fig.10.5: Load active power (KW)

Fig.10: The islanding action and load variations of a three-port system.

VII. CONCLUSION

The synchronous power controller shows more flexibility compared with the existing inertia emulation techniques, since it avoids the constraint between the damping and droop characteristics in the power regulating loop. Therefore, an outer P-f droop controller accompanied by a dedicated PLL is not needed for any operation stage, and the trade-off in designing the bandwidth of the droop loop low-pass filter is avoided. Besides, the fixed power control can be easily achieved in spite of grid frequency variations.

REFERENCES

1. M. A. Torres, L. A. Lopes, L. A. Moran, and J. R. Espinoza, "Selftuning virtual synchronous machine: A control strategy for energy storage systems to support dynamic frequency control," *IEEE Trans. Energy Convers.*,vol. 29, no. 4, pp. 833–840, Dec. 2014.
2. K. Rouzbehi, A. Miranian, A. Luna, and P. Rodriguez, "A generalized voltage droop strategy for control of multi-terminal DC grids," *IEEE Trans. Ind. Appl.*, vol. 51, no. 1, pp. 59–64, Jan./Feb. 2013.
3. J. Rocabert, A. Luna, F. Blaabjerg, and P. Rodri´ guez, "Control of power converters in AC microgrids," *IEEE Trans. Power Electron.*, vol. 27,no. 11, pp. 4734–4749, Nov. 2012.
4. J. M. Guerrero, J. C. Vasquez, J. Matas, L. G. De Vicuitna, and M. Castilla, "Hierarchical control of droop-controlled AC and DC microgrids—A general approach toward

ISSN (Online) 2395-2717

International Journal of Engineering Research in Electrical and Electronic Engineering (IJEREEE)
Vol 3, Issue 3, March 2017

standardization," *IEEE Trans. Ind. Electron.*, vol. 58,no. 1, pp. 158–172, Jan. 2011.

5. Q. C. Zhong and G.Weiss, "Static synchronous generators for distributed generation and renewable energy," in *Proc. Power Syst. Conf. Expo.*, 2009,pp. 1–6.